The Effect of Virotherapy, Chemotherapy, and Immunotherapy to Immune System: Mathematical Modelling Approach

Aminatus Sa'adah[1, a)] Prihantini[2, b)] Bidayatul Masulah [3, c)]

[1]*Department of Informatics, Institut Teknologi Telkom Purwokerto, Purwokerto, Indonesia*
[2]*Department of Mathematics, Institut Teknologi Bandung, Bandung, Indonesia*
[3]*Mathematical Institute, Universiteit Leiden, Netherlands*

[a)]*email: aminatus@ittelkom-pwt.ac.id*
[b)]*email: titinprihantini4@gmail.com*
[c)]*email: bidayatul.masulah@umail.leidenuniv.nl*

Abstract

In the ever-evolving world of medical research and therapeutic interventions, the complex interaction among virotherapy, chemotherapy, and the immune system emerges as a fascinating field of investigation. Each of these treatments has its own advantages and disadvantages. In this study, a mathematical model was developed that describes the interaction of the immune system, tumor cells, and normal cells when the three types of therapy are applied to cancer patients. Numerical simulations of eight treatment strategies (a combination of three types of therapy) were carried out to determine how much the concentration of immune cells, tumor cells, and normal cells decreased as a result of the treatment. Based on the numerical simulations performed, the application of the three types of therapy provided the greatest reduction (99%) in the concentration of tumour cells but also provided a significant reduction (68%) in the concentration of immune cells in the body.

Keywords: cancer, chemotherapy, immunotherapy, mathematical modelling, tumor, virotherapy

Introduction

In the ever-evolving landscape of medical research and therapeutic interventions, the intricate interplay between virotherapy, chemotherapy, and the immune system stands as a captivating subject of investigation [1][2]. As humanity continues its relentless quest to combat formidable diseases such as cancer, a deeper understanding of the multifaceted interactions within the body becomes paramount. It is within this context that the present paper emerges, delving into the intricate dynamics between virotherapy, chemotherapy, and the immune system through the lens of mathematical modeling.

The confluence of virotherapy and chemotherapy has redefined the therapeutic landscape, presenting both novel opportunities and complex challenges. Virotherapy, harnessing the power of viruses to selectively target and destroy cancer cells, has emerged as a groundbreaking approach with immense potential [1][3]. In tandem, chemotherapy, with its systemic impact on rapidly dividing.

Cells, has remained a cornerstone of cancer treatment regimens [2][4]. However, the dual effects of these modalities on the immune system, while undoubtedly pivotal, present an intricate puzzle that demands systematic unraveling.

Central to this discourse is the immune system, an orchestrator of defense that navigates an intricate network of interactions to maintain equilibrium within the body. The convergence of virotherapy and chemotherapy upon this intricate system introduces a multitude of variables that influence the delicate balance between immune suppression and activation [5]. It is within this context that mathematical modeling emerges as an indispensable tool, offering a platform to simulate and comprehend the intricate dynamics governing these treatment modalities' impact on immune response [6]. Mathematical models are widely used to study the dynamics of diseases including tuberculosis [7], HPV [8], dengue [9], and many more.

This paper embarks on a comprehensive exploration of the multifaceted relationships between virotherapy, chemotherapy, and the immune system, utilizing mathematical models as a conduit for inquiry [1][5]. By integrating empirical data, theoretical insights, and computational simulations, we seek to unravel the intricate mechanisms that underlie the observed effects on immune cell populations, cytokine cascades, and the overall tumor microenvironment [10]. Through rigorous analysis, we aim to decipher the nuances of immune response modulation induced by these therapeutic strategies, shedding light on potential synergies or antagonisms that might arise.

As we navigate through the pages of this paper, we shall traverse the landscapes of virotherapy and chemotherapy, dissecting their individual and combined effects on immune cells, their proliferation, activation, and response kinetics [5].Our mathematical framework, constructed with meticulous attention to biological plausibility, shall serve as a virtual laboratory, facilitating the exploration of diverse scenarios and parameter spaces that might not be easily accessible through experimentation alone [6].

In the grand tapestry of medical progress, this paper endeavors to contribute a thread of insight into a dynamic field that holds the promise of transforming lives. By harnessing the power of mathematical modeling we aspire to provide a deeper comprehension of the intricate interplay between virotherapy, chemotherapy, and the immune system. Ultimately, it is our hope that this endeavor will inspire further research, illuminate novel therapeutic avenues, and bring us closer to the day when the ravages of cancer can be met with strategies of unparalleled precision and efficacy [10]. In this study, a mathematical model was developed that describes the interaction of the immune system, tumor cells, and normal cells when the three types of therapy are applied to cancer patients. Numerical simulations of eight treatment strategies (a combination of three types of therapy) were carried out to determine how much the concentration of immune cells, tumor cells, and normal cells decreased as a result of the treatment.

Mathematical Model

In this research, the mathematical model of tumor growth is developed based on [6] and [11]. Different from [6], the present model added immunotherapy as a cancer treatment. Hence, there are three treatment types: chemotherapy, virotherapy, and immunotherapy. The biological states of the model are listed in the following:

E: Immune cells concentration per liter of blood (cell/L);
U: Uninfected tumor cells concentration per liter of blood (cell/L);
I: Infected tumor cells concentration per liter of blood (cell/L);
N: Normal cells concentration per liter of blood (cell/L);

V: Virotherapy concentration per liter of blood (virus/L);
C: Chemotherapy concentration per liter of blood (mg/L);
L: IL-2 concentration per liter of blood (IU/L);
and control variables are:
v_L: Amount of IL-2 injected per day per liter of blood $(\text{IU/(L} \times \text{day)})$;
v_M: Amount of Doxorubicin injected per day per liter of blood $(\text{mg/(L} \times \text{day)})$.

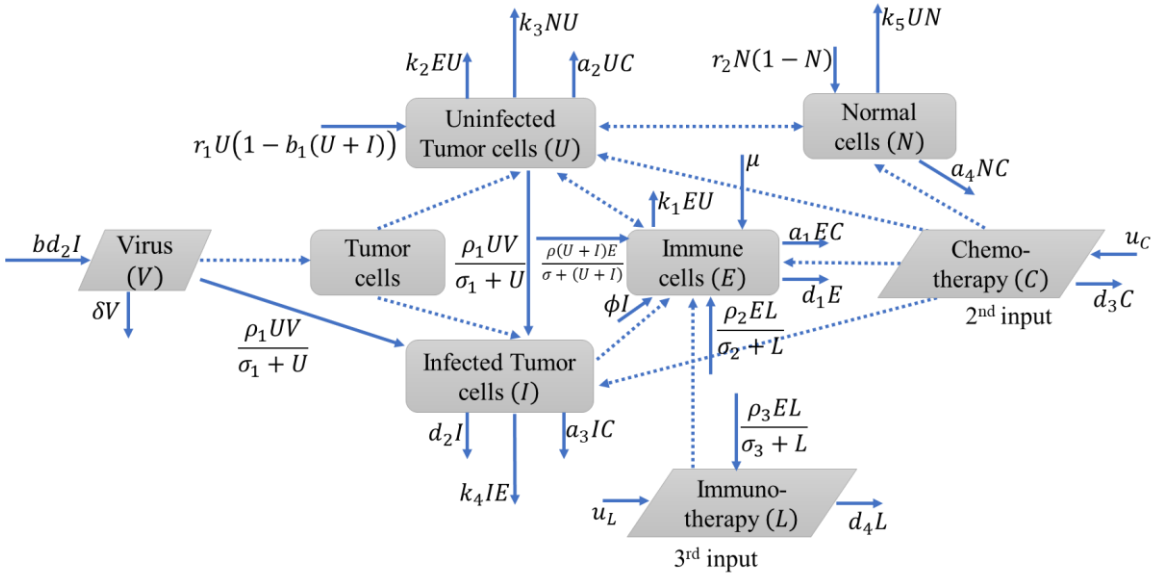

Figure 1. The diagram of immune-tumor-normal cells in the presence of virotherapy, chemotherapy, and immunotherapy.

The interaction between immune system, tumor cells, and normal cells when given viro-chemo-immunotherapy is given in the Figure 1. The model is develop based on some assumptions. Injections of IL-2 are classified as immunotherapy. Tumor cells are eradicated by viruses, whereas any type of cells is destroyed by chemotherapy drugs. The population of infected tumor cells determines how strongly the immune system reacts to the virus at the rate of ϕI. As the density of tumor cells that are infected rises, the number of viruses grows. The source of the virus is the infected cells since they release free virions into the tissue space at the rate of $d_2 I$. Tumor cells multiply more rapidly than normal cells do. The Michaelis-Menten term $\frac{\rho(U+I)E}{\sigma+(U+I)}$ describes how the presence of tumor cells increases the immune response. The term $\frac{(\rho_1 UV)}{\sigma_1+U}$ refers to the virus's capability to infect tumor cells. We discuss tumor-virus-specific immune responses. These viruses can be altered to have beneficial characteristics such as decreasing the capacity of tumor cells to infect healthy cells and enabling them to deliver therapeutic payloads only to tumors and infected tumor cells by generating immune-stimulating cells [6][11].

In Eq. (1), the term μ represents the constant proliferation rate of immune cells already present in our body. The term $\frac{\rho(U+I)E}{\sigma+(U+I)}$ describes tumor-specific immune response in the form of Michaelis–Menten term. The immune cell population decreases due to the natural decay rate $d_1 E$, tumor-specific immune decay rate $k_1 EU$, and kill rate due to drug administration $a_1 EC$. In Eqs. (2) and (3

the tumor growth rate is represented by the term $r_1U\big(1-b_1(U+I)\big)$. The virus will infect the tumor cell so that the uninfected tumor cells will become infected tumor cells with the infection rate $\frac{\rho_1 UV}{\sigma_1+U}$. The uninfected tumor cells population decrease due to killed by immune cells with decay rate k_2EU, interact with normal cell with decay rate k_3NU, and drug administration a_2UC. The infected tumor cells decrease due to killed by immune cells k_4IE and drug administration a_3IC.

In Eq. (4), the normal cells grow with rate $r_2N(1-N)$ and decay due to interact with uninfected tumor cells with rate k_5U and killed by drug administration a_4NC. In Eq. (5), the virus proliferates at a rate bd_2I and deactivate in the body tissue by δV. The loss of free virus due to infection of the uninfected tumor cells with rate $\left(\frac{\rho_1 UV}{\sigma_1+U}\right)$. In Eq. (6), the dose of chemotherapeutic drug is given with rate u_C and decrease with the decay rate d_3C. In Eq. (7), the concentration of IL-2 is given with rate u_L and decrease by natural decay rate d_3L. The immune cells and IL-2 interactions result in a natural growth rate for both ($\frac{\rho_2 LE}{\sigma_2+L}$ and $\frac{\rho_3 LE}{\sigma_3+L}$ respectively).

The mathematical of tumor growth given in the system (1) below:

$$\frac{dE}{dt}=\mu+\frac{\rho(U+I)E}{\sigma+(U+I)}-d_1E-k_1EU-a_1EC+\phi I+\frac{\rho_2 EL}{\sigma_2+L} \tag{1}$$

$$\frac{dU}{dt}=r_1U\big(1-b_1(U+I)\big)-\frac{\rho_1 UV}{\sigma_1+U}-k_2EU-k_3NU-a_2UC \tag{2}$$

$$\frac{dI}{dt}=\frac{\rho_1 UV}{\sigma_1+U}-d_2I-k_4IE-a_3IC \tag{3}$$

$$\frac{dN}{dt}=r_2N(1-N)-k_5UN-a_4NC \tag{4}$$

$$\frac{dV}{dt}=bd_2I-\frac{\rho_1 UV}{\sigma_1+U}-\delta V \tag{5}$$

$$\frac{dC}{dt}=u_C-d_3C \tag{6}$$

$$\frac{dL}{dt}=u_L+\frac{\rho_3 EL}{\sigma_3+L}-d_4L \tag{7}$$

$E(t),U(t),I(t),N(t),V(t),C(t),L(t)\geq 0$ for all $t\geq 0$ with the initial condition is $E(0)=E_0,U(0)=U_0,I(0)=I_0,N(0)=N_0,V(0)=V_0,C(0)=C_0,L(0)=L_0$. The description of the model parameters is given in Table 1.

Table 1. Description and value of the parameters of the proposed model

Parameters	Description	Values	Unit
μ	Constant source rate of immune cells existing in the body	0.05 [6]	Cell/L.day^{-1}
ρ	Maximum immune cell recruitment by tumor cells	1 [6]	Day^{-1}
σ	Half-saturation for the proliferation term	0.4 [6]	Cell/ L
ϕ	Immune response specific to viruses	0.1 [6]	L^{-1}.day^{-1}
r_1	Intrinsic tumor growth rate	0.45 [6]	Day^{-1}
r_2	Growth rate of normal cell	0.35 [6]	Day^{-1}
$1/b_1$	Tumor population carrying capacity	2/3 [6]	Cell/ L
ρ_1	Infection rate	0.4 [6]	Day^{-1}
ρ_2	Proliferation coefficient of immune cells	0.4 [12]	Day^{-1}

Parameters	Description	Values	Unit
ρ_3	IL-2 production rate from immune cells	0.2 [12]	Day^{-1}
σ_1	Michaelis–Menten constants	0.2 [6]	Cell/ L
σ_2	Saturation constant of proliferation term of effector cells	1 [12]	IU. L^{-1}
σ_3	Saturation constant of source term of IL-2	1 [12]	IU. L^{-1}
δ	Virus deactivation in the body tissue	0.001 [6]	Day^{-1}
d_1	Natural decay rate of immune cells	0.2 [6]	Day^{-1}
d_2	Natural death rate of infected tumor cells	0.01 [6]	Day^{-1}
d_3	Natural decay rate of drug	0.05 [6]	Day^{-1}
d_4	IL-2 self-elimination rate	0.1 [12]	Day^{-1}
a_1	Immune cell decay rate induced by chemotherapy toxicity	0.2 [6]	$Cell^{-1}.day^{-1}$
a_2	Uninfected tumor cell kill rate due to drug	0.5 [6]	$Cell^{-1}.day^{-1}$
a_3	Infected tumor cell kill rate due to drug	0.1 [6]	$Cell^{-1}.day^{-1}$
a_4	Normal cells kill rate due to drug	0.2 [6]	$Cell^{-1}.day^{-1}$
k_1	Decay rate of immune cells due to uninfected tumor cells	0.2 [6]	$Cell^{-1}.day^{-1}$
k_2	Uninfected tumor decay rate induced by immune	0.3 [6]	$Cell^{-1}.day^{-1}$
k_3	Decay rate of uninfected tumor cells due to normal cells	0.2 [6]	$Cell^{-1}.day^{-1}$
k_4	Infected tumor decay rate induced by immune cells	0.05 [6]	$Cell^{-1}.day^{-1}$
k_5	Decay rate of normal cells due to uninfected tumor cells	0.25 [6]	$Cell^{-1}.day^{-1}$
b	Virus burst size	Varied	Day^{-1}
u_C	Dose of chemotherapy drug injected per day per liter of blood	Varied	(mg/ (L.Day)
u_L	Amount of IL-2 injected per day per liter of blood	Varied	(IU/(L.Day))

Dynamical Analysis of the Model

In this section, we will analyze the stability of the equilibrium of system (1). The model has two equilibrium points, namely tumor-free equilibrium and tumor equilibrium. The equilibrium point of the model is obtained when there is no rate of change in the model, that is

$$\frac{dE}{dt} = \frac{dU}{dt} = \frac{dI}{dt} = \frac{dN}{dt} = \frac{dV}{dt} = \frac{dC}{dt} = \frac{dL}{dt} = 0.$$

The tumor-free equilibrium points of the system (1) is $P_0 = \left\{E = \frac{\mu}{d_1}, U = 0, \mathrm{I} = 0, N = 1, V = 0, C = 0, L = 0\right\}$, while the tumor equilibrium point of the system (1) consists of a high-dimensional non-linear system so it is difficult to obtain a balanced solution analytically.

Theorem 1. The tumor-free equilibrium points P_0 is asymptotically stable if $\frac{r_1 d_1}{k_3 d_1 + k_2 \mu} < 1$ and $\frac{k_4 \mu}{d_1 d_2} < 1$.

Proof. The tumor-free equilibrium points of the system (1) is $P_0 = \left\{E = \frac{\mu}{d_1}, U = 0, \mathrm{I} = 0, N = 1, V = 0, C = 0, L = 0\right\}$. The local stability of the tumor-free equilibrium point P_0 is obtained by linearizing

the system (1) around the equilibrium point P_0 using the Jacobi matrix $J_0 = \frac{\partial \boldsymbol{F}}{\partial \mathbf{x}}\Big|_{P_0}$ where $\boldsymbol{F} = \left\{\frac{dE}{dt}, \frac{dU}{dt}, \frac{dI}{dt}, \frac{dN}{dt}, \frac{dV}{dt}, \frac{dC}{dt}, \frac{dL}{dt}\right\}$ and $\mathbf{x} = \{E, U, I, N, V, C, L\}$. Based on system (1), we obtained Jacobian matrix J_0 in around the tumor-free equilibrium point P_0 as follows:

$$J_0 = \begin{pmatrix} -d_1 & \frac{\rho\mu}{d_1\sigma} - \frac{k_1\mu}{d_1} & \frac{\rho\mu}{d_1\sigma} + \phi & 0 & 0 & -\frac{a_1\mu}{d_1} & \frac{\rho_2\mu}{d_1\sigma_2} \\ 0 & r_1 - \frac{k_2\mu}{d_1} - k_3 & 0 & 0 & 0 & 0 & 0 \\ 0 & 0 & -\frac{k_4\mu}{d_1} - d_2 & 0 & 0 & 0 & 0 \\ 0 & -k_5 & 0 & -r_2 & 0 & -a_4 & 0 \\ 0 & 0 & bd_2 & 0 & -\delta & 0 & 0 \\ 0 & 0 & 0 & 0 & 0 & -d_3 & 0 \\ 0 & 0 & 0 & 0 & 0 & 0 & \frac{\rho_3\mu}{d_1\sigma_3} - d_4 \end{pmatrix}$$

The eigen values of the Jacobi matrix J_0 are $\lambda_1 = -r_2$, $\lambda_2 = -d_1$, $\lambda_3 = -d_3$, $\lambda_4 = -\delta$, $\lambda_5 = -\left(d_4 + \frac{\mu\rho_3}{d_1\sigma_3}\right)$, $\lambda_6 = r_1 - \left(k_3 + \frac{k_2\mu}{d_1}\right)$, and $\lambda_7 = \frac{k_4\mu}{d_1} - d_2$. The model in Eq. (1) will be asymptotically stable if all of the eigen values are negative ($\lambda < 0$). The sixth eigen value λ_6 will be negative if $\frac{r_1 d_1}{k_3 d_1 + k_2\mu} < 1$ and the seventh eigen value λ_7 will be negative if $\frac{k_4\mu}{d_1 d_2} < 1$. Hence, the tumor-free equilibrium will asymptotically stable if $\frac{r_1 d_1}{k_3 d_1 + k_2\mu} < 1$ and $\frac{k_4\mu}{d_1 d_2} < 1$. ■

Results and Discussion

Analysis of the dynamics of the mathematical model of tumor growth that has been built is done numerically. Numerical simulations were carried out in as many as eight strategies based on a combination of three treatments, namely virotherapy (b), chemotherapy (u_C), and immunotherapy (u_L), as follows:

Scenario 1: without treatment ($b = 0, u_C = 0, u_L = 0$),
Scenario 2: virotherapy only ($b \neq 0, u_C = 0, u_L = 0$),
Scenario 3: chemotherapy only ($b = 0, u_C \neq 0, u_L = 0$),
Scenario 4: immunotherapy only ($b = 0, u_C = 0, u_L \neq 0$),
Scenario 5: chemotherapy and immunotherapy ($b = 0, u_C \neq 0, u_L \neq 0$),
Scenario 6: virotherapy and immunotherapy ($b \neq 0, u_C = 0, u_L \neq 0$),
Scenario 7: virotherapy and chemotherapy ($b \neq 0, u_C \neq 0, u_L = 0$), and
Scenario 8: virotherapy, chemotherapy, and immunotherapy at once ($b \neq 0, u_C \neq 0, u_L \neq 0$).

The solution for the proposed model in the system (1) is obtained using the 4th order Runge-Kutta algorithm (RK-4) by using the ode45 solver in MATLAB. The stability and convergence of the fourth-order Runge-Kutta algorithm can be seen in [13]. The initial value of the compartment used for the simulation is E_0 = 0.2; U_0 = 0.05; I_0 = 0.1; N_0 = 0.6; V_0 = 0.001; C_0 = 0.001; L_0 = 0.001. While the parameter values refer to Table 1. The dynamics of immune cells, tumor cells, and normal cells resulting from the numerical simulation of the eight strategies are shown in Figure 2-Figure 5.

Figure 2 shows that immune cell concentrations will reach different peaks for the eight treatment strategies. The highest peak of immune cells occurred in the application of Scenario 6, namely viro-immunotherapy. Scenario 7 (viro-chemotherapy) resulted in the lowest number of immune cell concentrations at the end of the simulation time. Figure 3 and Figure 4 displays the tumor cell

concentrations for the eight strategies. The strategies that provided the greatest reduction in the concentration of uninfected tumor cells were Scenario 7 and Scenario 8. Meanwhile, those that provided the greatest reduction in the concentration of infected tumor cells were strategies 5 and Scenario 6. Figure 5 displays normal cell concentrations based on the implementation of the eight strategies. At the end of the simulation time, the highest concentration of normal cells was obtained from the application of Scenario 6. Meanwhile, the largest decrease in the concentration of normal cells occurred during the application of Scenario 3.

In summary, the decrease in the concentrations of immune cells, tumor cells, and normal cells at the end of the simulation is given in Table 2 and Table 3. Based on Table 3, Scenario 8 (a combination of three treatments at once) provided the most significant reduction in tumor cell concentration at the end of the simulation time, which was 99.33%. However, Scenario eight significantly impacted the concentration of immune cells at the end of the simulation time, namely 68.68% and 18.85% of normal cells. Scenario 2 (virotherapy only) is the Scenario that least decreases the number of immune cells at the end of the simulation time, which is 25.68%. However, Scenario two was only able to reduce the concentration of tumor cells by 21.90%.

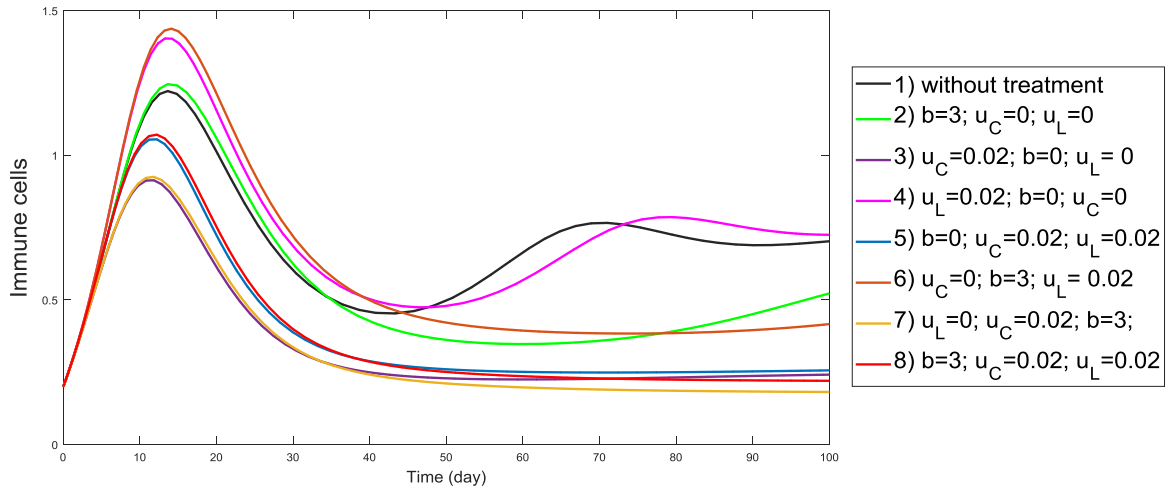

Figure. 2. The dynamics of immune cells for different treatment Scenario

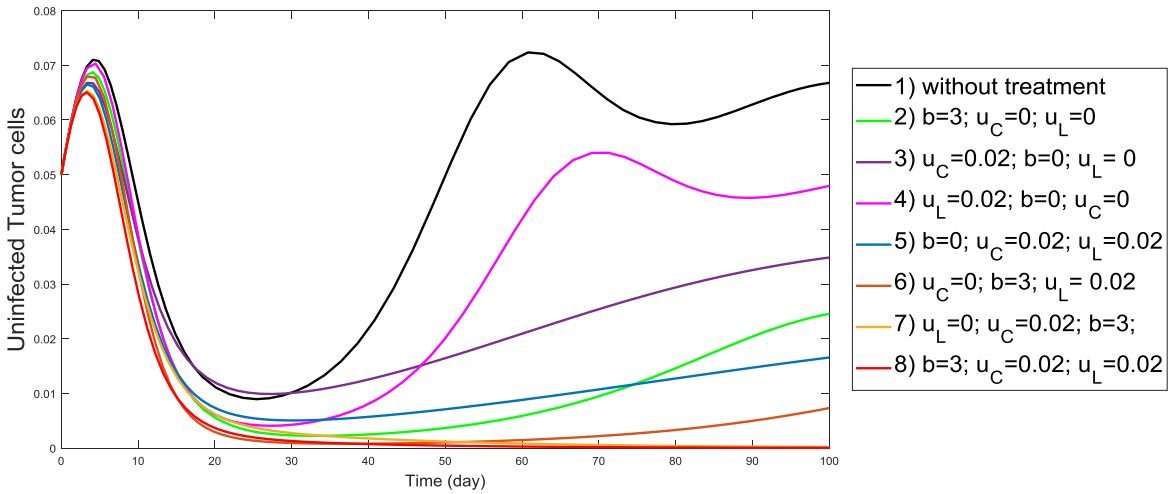

Figure. 3. The dynamics of uninfected tumor cells for different treatment Scenario

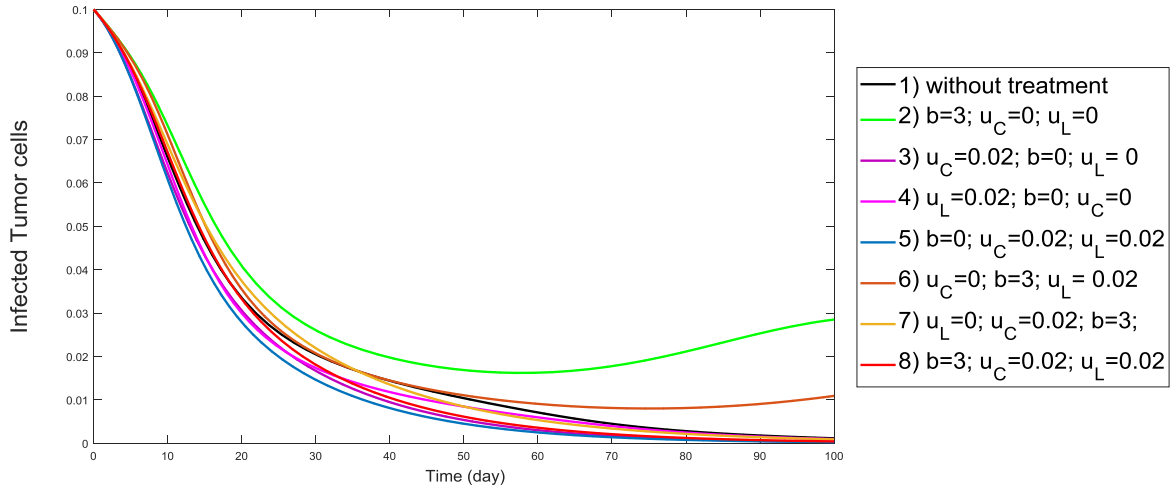

Figure 4. The dynamics of infected tumor cells for different treatment Scenario

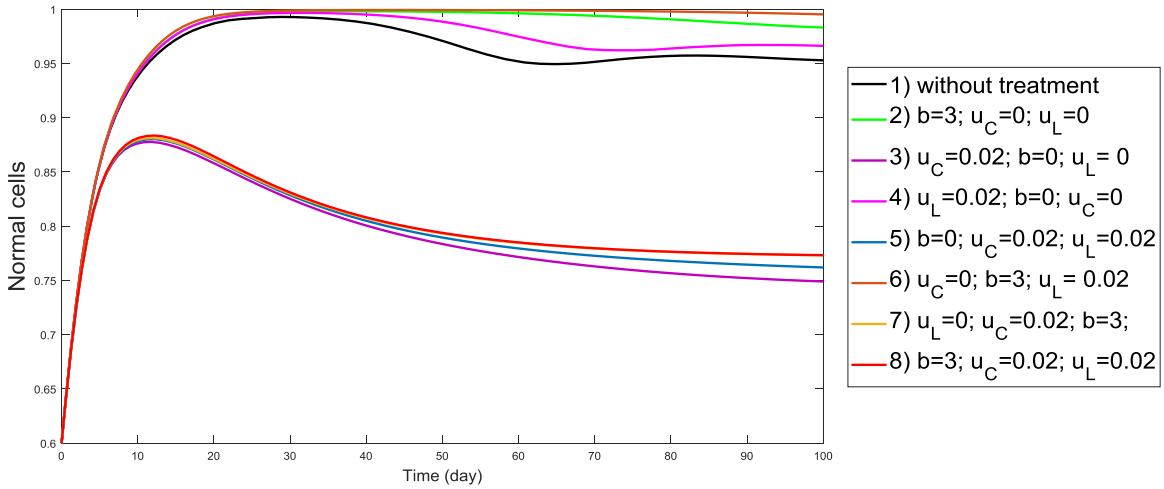

Figure 5. The dynamics of normal cells for different treatment Scenario

Table 2. Comparison of cell concentration at the end of the simulation

	Immune cells (cell/L)	Tumour cells (cell/L)	Normal cells (cell/L)
Scenario 1	0.7025	0.067927	0.9529
Scenario 2	0.5221	0.05305	0.9832
Scenario 3	0.2413	0.0351368	0.749
Scenario 4	0.7248	0.0489074	0.9663
Scenario 5	0.2561	0.0168	0.762
Scenario 6	0.4161	0.0182	0.9953
Scenario 7	0.1814	0.0011	0.7732
Scenario 8	0.22	4.5697e-04	0.7733

Table 3. Comparison of the percentage of cell reduction in each Scenario

	Immune cells (cell/lit)	Tumour cells (cell/lit)	Normal cells (cell/lit)
Scenario 2	25.68%	21.90%	-3.18%
Scenario 3	65.65%	48.27%	21.40%
Scenario 4	-3.17%	28.00%	-1.41%
Scenario 5	63.54%	75.27%	20.03%
Scenario 6	40.77%	73.21%	-4.45%
Scenario 7	74.18%	98.38%	18.86%
Scenario 8	68.68%	99.33%	18.85%

Furthermore, numerical simulations of variations in the doses of virotherapy, chemotherapy, and immunotherapy were carried out. Dynamics of immune cells, tumor cells, and normal cells based on the simulation results are given in Figures 6 –17. Figures 6-9 displays the dynamics of immune cells, uninfected tumor cells, infected tumor cells, and normal cells based on different chemotherapy doses. Based on Figure 6, the greater the dose of chemotherapy given, the less concentration of immune cells remains at the end of the simulation time. Likewise, in Figure 9, the greater the dose of chemotherapy given, the lower the concentration of normal cells remaining at the end of the simulation time. Based on Figures 7 and 8, the different doses of chemotherapy given produce the same output, namely a decrease in the overall concentration of tumor cells.

Figures 10–13 display the dynamics of immune cells, uninfected tumor cells, infected tumor cells, and normal cells based on different doses of IL-2 (immunotherapy). In figure 10, the greater the dose of immunotherapy given, the greater the concentration of immune cells remaining at the end of the simulation time. In figure 13, the different doses of immunotherapy have no effect on the concentration of immune cells during the simulation time. Based on Figures 11 and 12, immunotherapy was successful in reducing the concentration of tumor cells.

Figures 14–17 display the dynamics of immune cells, uninfected tumor cells, infected tumor cells, and normal cells for different values of virus burst. Variation in the value of the burst virus did not make a significant difference in immune cells, uninfected tumor cells, infected tumor cells, or normal cells. The dose of virotherapy given was able to reduce the overall number of tumor cells.

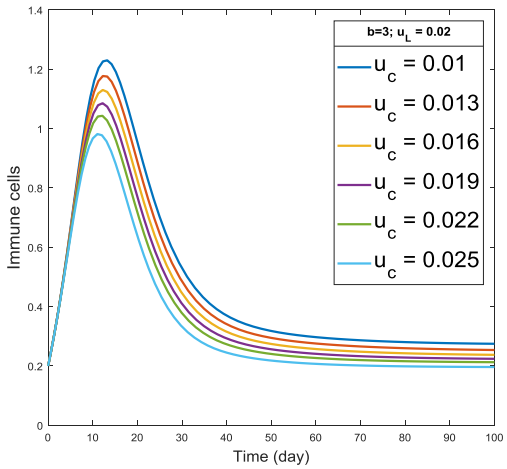

Figure 6. The dynamics of immune cells for different value of chemotherapy dose

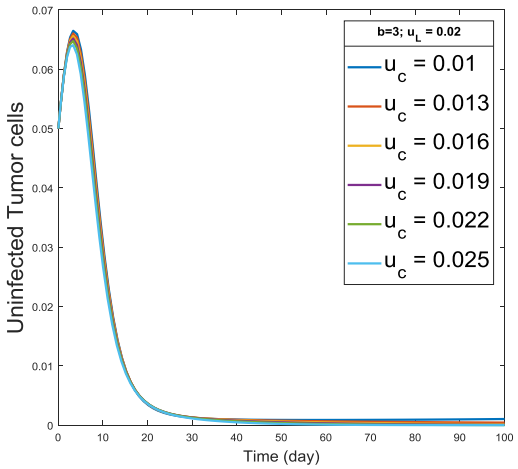

Figure 7. The dynamics of uninfected tumor cells for different value of chemotherapy dose

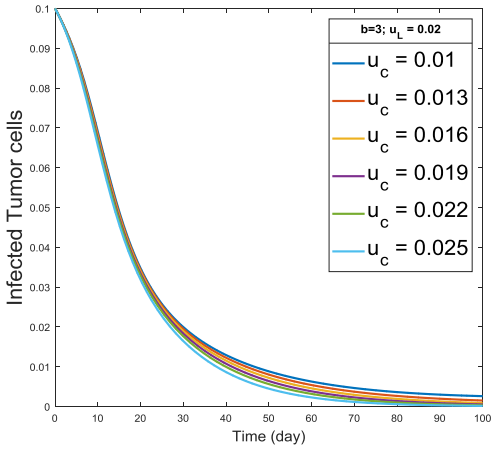

Figure 8. The dynamics of infected tumor cells for different value of chemotherapy dose

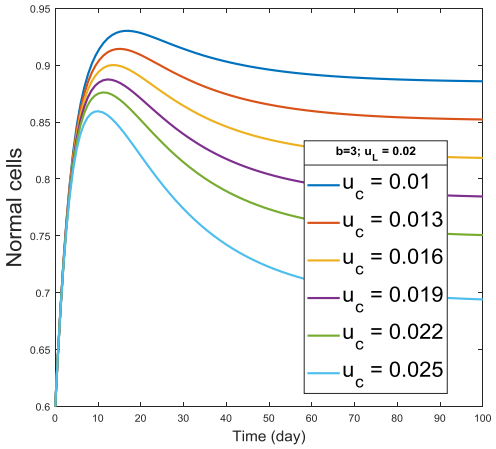

Figure 9. The dynamics of normal cells for different value of chemotherapy dose

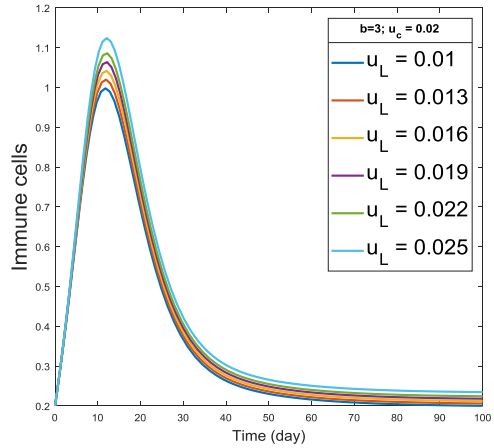

Figure 10. The dynamics of immune cells for different value of immunotherapy dose

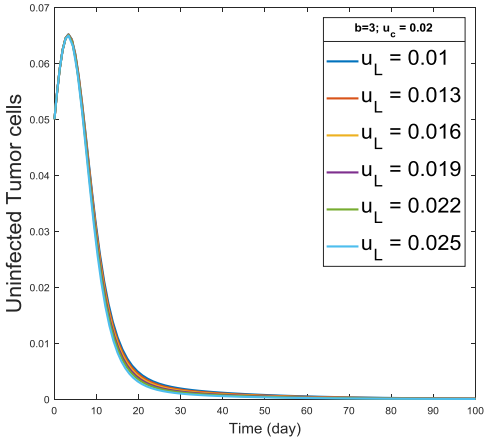

Figure 11. The dynamics of uninfected tumor cells for different value of immunotherapy dose

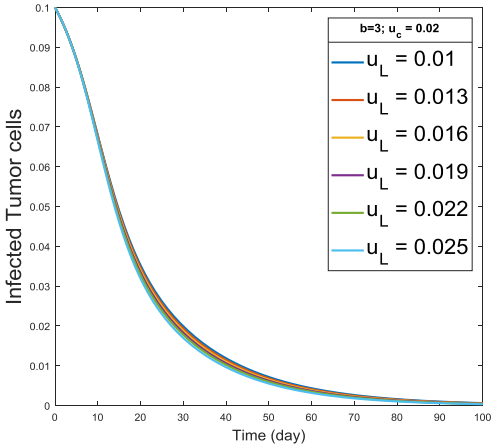

Figure 12. The dynamics of infected tumor cells for different value of immunotherapy dose

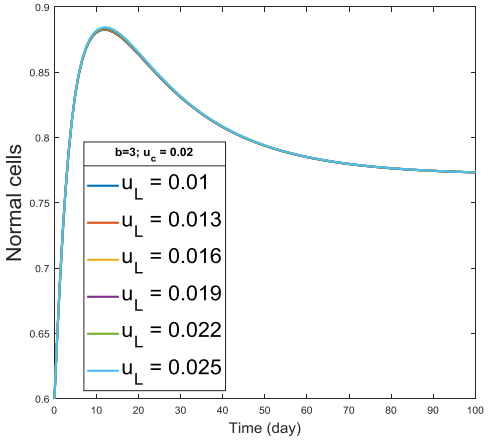

Figure 13. The dynamics of normal cells for different value of immunotherapy dose

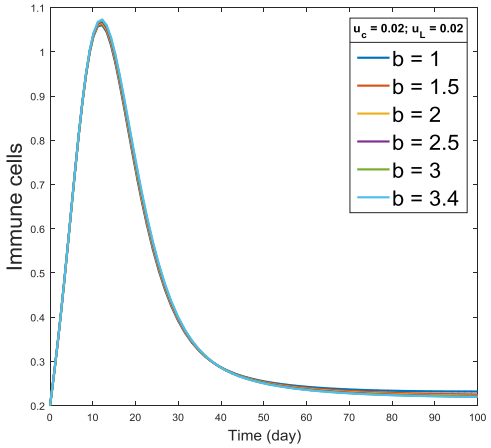

Figure 14. The dynamics of immune cells for different value of virus burst

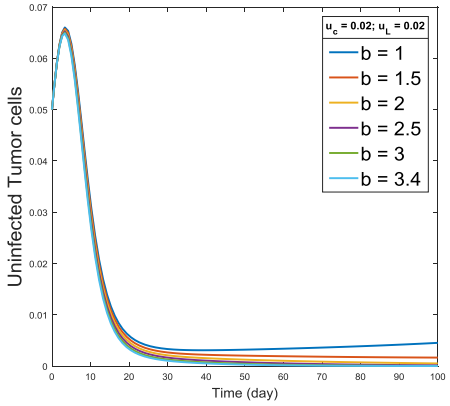

Figure 15. The dynamics of uninfected tumor cells for different value of virus burst

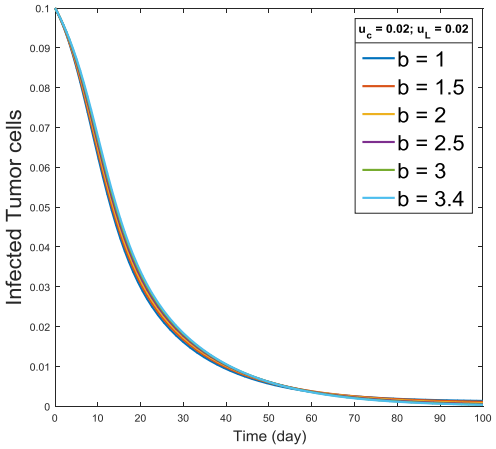

Figure 16. The dynamics of infected tumor cells for different value of virus burst

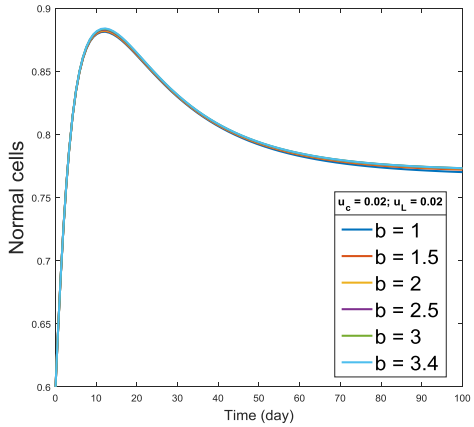

Figure 17. The dynamics of normal cells for different value of virus burst

Conclusion

A mathematical model of the interaction of the immune system, tumour cells and normal cells has been constructed in this study. The model built also involves three types of the latest cancer treatments, namely virotherapy, chemotherapy, and immunotherapy. Based on the numerical simulations performed, the application of the three types of therapy provided the greatest reduction (99%) in the concentration of tumour cells but also provided a significant reduction (68%) in the concentration of immune cells in the body. In other words, the goal of treatment, which is to eliminate tumor cells, can be achieved but has significant side effects on weakening the body's immune system. Therefore, further research is needed to measure the right dose that can eliminate tumor cells while keeping the immune system in a safe corridor.

References

[1] W. Lin, Y. Zhao, and L. Zhong, "Current strategies of virotherapy in clinical trials for cancer treatment," *J. Med. Virol.*, vol. 93, no. 8, pp. 4668–4692, 2021.

[2] G. M. Weir, R. S. Liwski, and M. Mansour, "Immune modulation by chemotherapy or

immunotherapy to enhance cancer vaccines," *Cancers (Basel).*, vol. 3, no. 3, pp. 3114–3142, 2011.

[3] M. M. Alam, S. Chowdhury, J. T. Chowdhury, M. M. Hasan, M. A. Ullah, and S. F. Ahmed, "Tumor treatment with chemo-virotherapy and MEK inhibitor: A mathematical model of Caputo fractional differential operator," *Alexandria Eng. J.*, vol. 71, pp. 173–183, 2023.

[4] D. Dahlgren and H. Lennernäs, "Review on the effect of chemotherapy on the intestinal barrier: Epithelial permeability, mucus and bacterial translocation," *Biomed. Pharmacother.*, vol. 162, p. 114644, 2023.

[5] A. Chen, I. Neuwirth, and D. Herndler-Brandstetter, "Modeling the Tumor Microenvironment and Cancer Immunotherapy in Next-Generation Humanized Mice," *Cancers (Basel).*, vol. 15, no. 11, p. 2989, 2023.

[6] A. Das, H. K. Sarmah, D. Bhattacharya, K. Dehingia, and K. Hosseini, "Combination of virotherapy and chemotherapy with optimal control for combating cancer," *Math. Comput. Simul.*, vol. 194, pp. 460–488, 2022.

[7] D. I. Amatillah, "Analisis sensitivitas dan kestabilan global model pengendalian tuberkulosis dengan vaksinasi, latensi dan perawatan infeksi." UIN Sunan Gunung Djati Bandung, 2021.

[8] S. H. Pratama, "Kestabilan Titik Ekuilibrium Endemik Pada Model SIS Transmisi Human Papillomavirus (HPV) Dengan Populasi Berbeda." UNIVERSITAS ISLAM NEGERI SULTAN SYARIF KASIM RIAU, 2020.

[9] N. Andiraja, S. Basriati, E. Safitri, R. Rahmadeni, and A. Martino, "Optimal Control of Vaccination for Dengue Fever in SIR Model," *KUBIK J. Publ. Ilm. Mat.*, vol. 7, no. 2, pp. 106–113, 2022.

[10] A. Yousef, F. Bozkurt, and T. Abdeljawad, "Mathematical modeling of the immune-chemotherapeutic treatment of breast cancer under some control parameters," *Adv. Differ. Equations*, vol. 2020, no. 1, pp. 1–25, 2020.

[11] P. Khalili and R. Vatankhah, "Studying the importance of regulatory T cells in chemoimmunotherapy mathematical modeling and proposing new approaches for developing a mathematical dynamic of cancer," *J. Theor. Biol.*, vol. 563, p. 111437, 2023.

[12] F. Dai and B. Liu, "Optimal control problem for a general reaction-diffusion tumor-immune interaction system of mixed immunotherapy and chemotherapy," *Eur. J. Control*, vol. 66, p. 100645, 2022.